EUROPHYSICS LETTERS 1 May 1996

Europhys. Lett., **34** (4), pp. 257-262 (1996)

Visualization of flow in multiple-scattering liquids

M. Heckmeier and G. Maret

Institut Charles Sadron (CRM-EAHP)
6 rue Boussingault, F-67083 Strasbourg Cedex, France

(received 24 January 1996; accepted in final form 11 March 1996)

PACS. 42.30−d – Imaging and optical processing.
PACS. 42.25Bs – Wave propagation, transmission and absorption.

Abstract. – We have performed quasi-elastic multiple-light-scattering experiments on a suspension of colloidal particles in Brownian motion into which a capillary with Poiseuille flow of the same suspension was inserted. We show that the time correlation function of the backscattered light, measured at various points on the sample surface, provides information on the position of the capillary and on the flow rate, demonstrating the possibility of imaging flow in turbid media under conditions of no static scattering contrast.

The field of multiple light scattering has rapidly evolved within the past decade after the discovery of coherent backscattering [1], [2]. By exploiting the principles of diffusing light, it has become possible, for example, to locate and image absorbing or transparent objects even when buried several optical transport mean free paths ([1]) l^* inside the multiple-scattering sample [3], [4]. Besides the static properties of multiple-scattered light, its time-dependent fluctuations have been widely studied [5]-[7]. The latter technique, which extends the usual Quasi-Elastic Light Scattering (QELS) from the regime of highly diluted systems [8] to turbid, concentrated suspensions, is sometimes called Diffusing Wave Spectroscopy (DWS). In DWS, the multiple scattering of light is described as a random walk of photons. On their tortuous way through the sample, the photons pick up time-dependent phase shifts on scattering from the particles in motion. The resulting time-dependent fluctuations of the speckle pattern of the scattered light probe the microscopic dynamics of the scatterers. Therefore, both diffusion constant and size of the colloidal particles undergoing Brownian motion can be determined. Similarly, time correlation functions from turbid suspensions undergoing flow provide quantitative information on shear gradients [9], [10]. This type of DWS requires homogeneous samples of randomly but uniformly distributed scatterers in motion.

Recently, Boas and coworkers [11] examined the case of a heterogeneous sample consisting of a spherical liquid inclusion inside a white solid material. Position-dependent measurements of the time autocorrelation function of the backscattered light provided a low-resolution image

([1]) The length over which the direction of propagation of diffusing light inside the sample is randomized.

of this hidden spherical cavity. In this experiment, there was contrast both in turbidity and in dynamics of scatterers between the buried object and the surrounding medium. Solid slab and included liquid had different photon transport mean free paths and hence, in principle, as in ref. [4], the included cavity could be imaged by analysing the static intensity profile of multiple-scattered light. In addition, liquid inclusion and solid surrounding generated dynamic and static speckle patterns, respectively, so that time fluctuations in the backscattered light provided additional contrast which was exploited to image the hidden liquid inclusion.

In this letter we report first DWS measurements on samples with a purely dynamic inhomogeneity. The sample, described in fig. 1, consists of a thin X-ray capillary (the object), filled with a turbid colloidal suspension and embedded in a large cell containing the very same suspension (the medium). The contrast which allows us to localize and visualize this hidden object is due to the different types of motion of scatterers inside and outside the object, inside laminar Poiseuille flow, outside purely Brownian motion (which of course also exists inside the capillary). Note that, the optical transport mean free path inside and outside the capillary being identical, static multiple light scattering does not provide contrast. As discussed below, photons having crossed the region of flow inside the capillary on their random path through the sample contribute in a different way to the decay of the time correlation function $g_1(t)$ than photons scanning regions of sole Brownian motion. The temporal decay of $g_1(t)$ thus depends on the positional coordinates with respect to the entrance and the exit point of diffusing light intensity of the sample. This allows to localize and visualize a dynamic inhomogeneity.

In quasi-elastic multiple light scattering, the motion of particles can be measured by exploiting the time autocorrelation function g_1 of the scattered electric field E: $g_1(t) = \langle E(0)E^*(t)\rangle/\langle|E(0)|^2\rangle$. In a backscattering experiment using a homogeneous semi-infinite liquid sample of suspended Brownian particles, g_1 has the well-known approximate form [7]

$$g_1(t) = \exp\Big[-\gamma\sqrt{\frac{3t}{2\tau_0}}\Big]. \tag{1}$$

Here $\tau_0 = (4Dk_0^2)^{-1}$ is the Brownian decay time, which can be measured in single scattering [8] (with D the diffusion constant of scatterers, k_0 the optical wave vector) and γ is a constant of order 2, related to the boundary conditions in the photon diffusion approach. In our geometry of a quasi–semi-infinite liquid sample with a buried capillary containing flow, the evaluation of $g_1(t)$ becomes more involved. In addition to the $\sqrt{t/\tau_0}$-decay of g_1 due to the stochastic Brownian motion there is a linear t-dependent contribution caused by the deterministic motion due to the flow [9], [10]. For our experimental case of a large capillary (diameter $d > l^*$) the characteristic time scale of this linear time dependence is $\tau_{\text{Flow}} = \sqrt{30}/(k_0 l^* \Gamma)$ where the average([2]) shear rate Γ is related to the flow rate Q by $\Gamma = 16Q/(\pi d^3)$. For the decay of the time correlation function not to be dominated by the Brownian motion of scatterers τ_{Flow} must be smaller than τ_0. Above the characteristic crossover time $\tau_c = \tau_{\text{Flow}}^2/4\tau_0$ between the two types of motion, g_1 is dominated by flow. The spatial distributions of both motions being inhomogeneous in our geometry (fig. 1), only *parts* of the photon cloud scan the additional dynamics due to flow. This contribution to the time correlation function is given by the probability that a photon crosses the capillary on its way through the sample. This probability is a non-trivial function of the capillary position and its diameter d and, similar to ref. [4], the relative contributions of the two types of motion to $g_1(t)$ depend on the location of the exit point of the detected light. In the case of a very thin capillary ($d < l^*$, at most one scattering event inside the tube) an expression for the position-dependent correlation function has been

([2]) The factor $\sqrt{30}$ in τ_{Flow} is valid for planar shear flow (ref. [9]) and for planar Poiseuille flow [12] but approximate in our case of cylindrical Poiseuille flow.

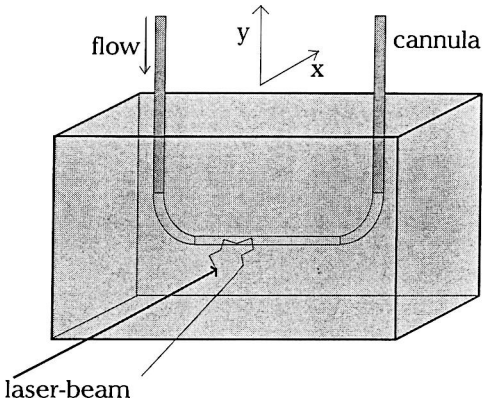

Fig. 1.

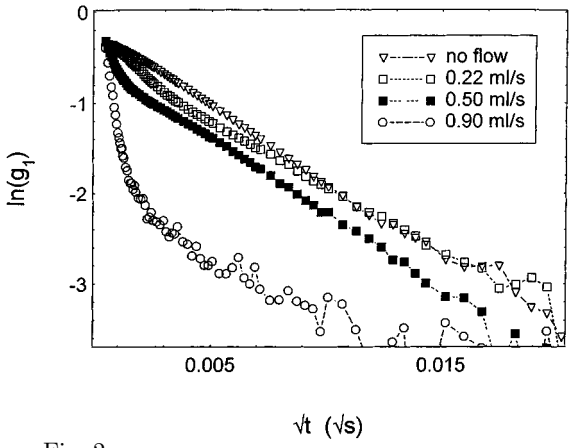

Fig. 2.

Fig. 1. – Sketch of the light scattering cell to realize spatially localized flow inside a turbid liquid. A large cell (5 cm × 4 cm × 2 cm) is completely filled with a concentrated colloidal suspension. Laminar Poiseuille flow of the same suspension occurs inside a pipe system consisting of an X-ray capillary (optical glass, length: 3 cm, diameter $d = 1.5$ mm, wall thickness: $\frac{1}{100}$ mm) and two heat-bent canullae sticked end on. A tube connected to the capillary delivers suspension from an elevated tank at flow rates controlled by its height. The capillary can be positioned at arbitrary x- and y-positions.

Fig. 2. – Time correlation functions for different flow rates. The capillary is placed at $x = 2.8\,l^*$ inside the cell and centred with respect to the incoming laser beam ($y = 0$).

derived [13]. Our case of $l^* < d$ (random walk of the photons also inside the capillary) has, to our knowledge, not been treated theoretically yet. Notwithstanding, our experiments show that valuable information can be obtained without knowledge of the exact functional dependence of the time correlation function. Simply by observing deviations from eq. (1) caused by the flow, we can localize the flow, visualize the capillary and, in principle, construct images.

We use a vertically polarized mono-mode Ar^+ laser beam ($\lambda = 514.5$ nm, waist ≈ 1 mm) incident on the sample cell as indicated in fig. 1. Approximately one coherence area of the backscattered light is collected onto a photomultiplier tube. In order to reduce the contribution of single scattering we detect depolarized light (VH-configuration). A PC-controlled correlator determines the autocorrelation function $g_2(t)$ of the scattered intensity. Since we work with pure liquid samples, all detected light contributes to a fluctuating speckle pattern and, in contrast to the work of Boas *et al.* [11], we are not concerned with the problem of non-ergodicity and ensemble averaging [14]. Hence, by using the Siegert relation [8] we obtain the field autocorrelation function $g_1(t)$. Our turbid liquid consists of a monodisperse suspension of polystyrene beads ($\tau_0 = 2.66 \times 10^{-4}$ s, diameter: 120 nm) in water, which were characterized by electron microscopy, single light scattering in the dilute regime and standard multiple-light-scattering experiments in backscattering and transmission geometry [7]. This provides $l^* = 69$ μm and $D = 3.55 \times 10^{-12}$ m^2/s.

First, we carefully checked that scattering contributions of the glass wall of the X-ray capillary are negligible. The capillary was positioned at the front side of the cell in contact with its wall (defined as $x = 0$, fig. 1) and vertically centred with respect to the incident laser beam ($y = 0$). The correlation function measured in this configuration without flow matched perfectly the correlation function obtained using the identical set-up but without X-ray capillary.

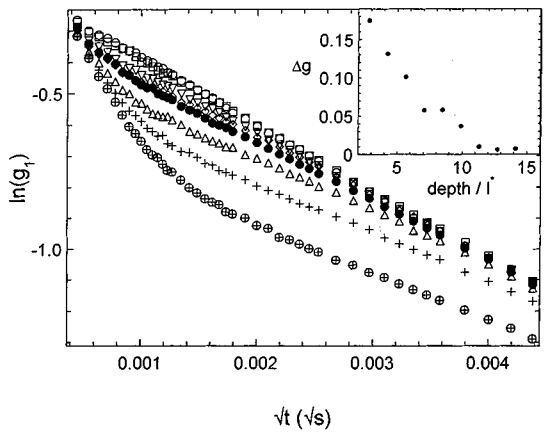

Fig. 3.

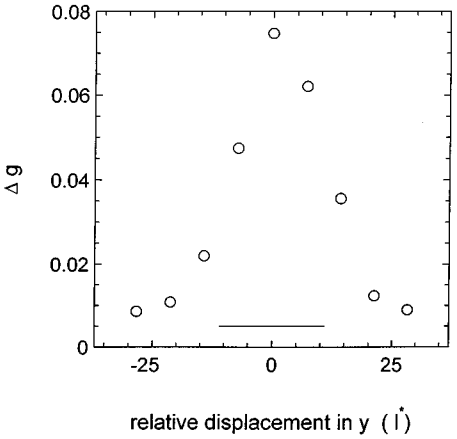

Fig. 4.

Fig. 3. – Time correlation functions for various positions of the capillary ($x = 2.8\,l^*$ ($\oplus$), $4.2\,l^*$ (+), $5.7\,l^*$ ($\triangle$), $7.1\,l^*$ ($\bullet$), $8.5\,l^*$ ($\diamond$), $9.9\,l^*$ ($\triangledown$), $11.3\,l^*$ ($\square$), $y = 0$) compared to the case of no flow ($\circ$). Inset: The maximum difference Δg of these correlation functions with respect to the Brownian case as a function of the x-position of the capillary.

Fig. 4. – For a fixed x-position of $7.1\,l^*$ inside the cell, Δg is shown as a function of the y-position of the flow. The width of the capillary is indicated by the line.

Figure 2 demonstrates the sensitivity of our method to the flow rate inside the capillary embedded in the Brownian environment. For the case of no flow, $g_1(t)$ has the square-root time dependence as expected from eq. (1). Small short time deviations from $\sqrt{t}$ are due to the finite size of the incident laser beam. With increasing flow rate, increasing deviations from eq. (1) are observed at small and intermediate times, whereas all curves show a tendency to merge at long times. Note that even for the lowest flow rate $Q = 0.22$ ml/s the crossover time $\tau_c = 2.03 \times 10^{-7}$ s is very short and hence the short-time Brownian regime ($t < \tau_c$) is not visible in these data. τ_c is in the range of our shortest measurable correlation time, so the flow is most sensitively probed by the short-time decay of $g_1(t)$. This is obvious from the general feature of DWS that the short-time decay of $g_1(t)$ is dominated by long paths and *vice versa* [7]. Long paths have a higher probability of crossing the capillary than short paths. For large times, the decay in $g_1(t)$ is governed by Brownian motion because most of the short paths have not crossed the capillary, so the curves tend to coincide for all measured flow rates. If the depth of the capillary inside the turbid liquid is known, this measurement provides a method to measure flow rates.

Next, we examined up to which in-depth position x of the capillary a flow contribution to the decay of the measured time correlation function of the backscattered light can be detected. Figure 3 shows $g_1(t)$ at different depths x of the capillary, at $y = 0$ and $Q = 0.50$ ml/s. Up to $x = 11.3\,l^*$, we observe a clear deviation of the correlation function from the Brownian case at short and intermediate times. This can be explained as above by the time (t)-path (s) relation $t = 4\tau_0(l^*/s)$ in DWS [7]. Short times correspond to long paths, so at short times a higher fraction of the photon cloud inside the turbid liquid sees the tube and contributes to the non-Brownian decay in time correlations. At larger times the curves come closer and eventually merge, which again indicates the less important contribution from short paths to the linear time decay of g_1 due to flow. Consequently, for increasing depth of the flow, the curves converge at progressively shorter times to the form of $g_1(t)$ given by eq. (1).

The inset of fig. 3 shows the maximum difference Δg between the measured correlation functions and the case without flow, plotted against the x-position of the flow inside the container. This plot reveals a clear monotonic variation of Δg with x, illustrating the decreasing contribution of the flow to the backscattered light with increasing x-position of the capillary. We find a measurable contrast up to $x = 11\,l^*$, which demonstrates the possibility of flow imaging to depths about an order of magnitude larger than the photon transport mean free path. The rapid decay in Δg can be related to the phase shifts picked up by a photon on its diffusing path to the centre of the capillary and back to the front of the cell: The distance $2x + d$ which corresponds to a typical path length $(2x + d)^2/l^*$ results in a characteristic time $\tau_{\text{Path}} = 4\tau_0((l^*)^2/(2x + d)^2)$ above which the decay of $g_1(t)$ is governed by the Brownian motion of the scatterers. To measure a contribution of flow to the decay of g_1, τ_{Path} has to be larger than the crossover time τ_c, which provides a time range $\tau_c \leq t \leq \tau_{\text{Path}}$ for the application of our method. As is evident from fig. 3, this time window is very large for small depths x and becomes rapidly smaller with increasing x due to the decrease of τ_{Path} ([3]). This goes along with a decrease in the amplitude of the flow effect because of the decreasing photon density crossing the tube, as in ref. [4].

Finally, we show in fig. 4 the maximum dynamic contrast Δg, measured for a fixed x-position of $7.1\,l^*$ as a function of the y-position of the capillary. For the sake of comparison the width of the capillary is also shown. The figure clearly demonstrates the feasibility of making the hidden tube visible. For $y = 0$, there is a well-defined maximum in Δg. A vertical displacement by about one radius of the capillary results in a strong decay of Δg to very small values. The direct correlation between the vertical flow position and the change in Δg allows in principle the construction of an image of flow. This is a special feature of the case $x \leq d$. For $d \ll x$, however, as in ref. [4], we expect that only the centre of gravity of the tube could be located.

In conclusion, we demonstrate that a measurement of the temporal fluctuations of the multiple-scattered light provides a possibility of localizing and visualizing a dynamic imhomogeneity buried up to several optical transport mean free paths inside the sample. Studying flow in a capillary surrounded by suspended Brownian particles, a window in correlation times for the applicability of this method is found. It depends on the flow rate and on the depth of the buried flow. The described principle should allow the imaging of any object undergoing a distinct motion with respect to the surrounding medium. It, therefore, could be used in various applications, particularly in biology and medicine.

***

We are indebted to R. MAYNARD and D. BICOUT for fruitful discussions. MH acknowledges financial support by the Deutscher Akademischer Austauschdienst (DAAD) through the HSPII/AUFE-program.

REFERENCES

[1] VAN ALBADA M. P. and LAGENDIJK A., *Phys. Rev. Lett.*, **55** (1985) 2692.
[2] WOLF P. E. and MARET G., *Phys. Rev. Lett.*, **55** (1985) 2696.
[3] BERKOVITS R. and FENG S., *Phys. Rev. Lett.*, **65** (1990) 3120.
[4] DEN OUTER P. N., NIEUWENHUIZEN TH. M. and LAGENDIJK A., *J. Opt. Soc. Am. A*, **10** (1993) 1209.
[5] MARET G. and WOLF P. E., *Z. Phys. B*, **65** (1987) 409.

([3]) In this qualitative picture, setting $\tau_c = \tau_{\text{Path}}$ allows to estimate an upper limiting distance x of about $70\,l^*$, which is of the same order of magnitude as our data.

[6] Pine D. J., Weitz D. A., Chaikin P. M. and Herbolzheimer E., *Phys. Rev. Lett.*, **60** (1988) 1134.

[7] Pine D. J., Weitz D. A., Wolf P. E., Maret G., Herbolzheimer E. and Chaikin P. M., in *Scattering and Localization of Classical Waves in Random Media*, edited by Ping Sheng (World Scientific, London, Singapore) 1989.

[8] Berne B. J. and Pecora R., *Dynamic Light Scattering* (Wiley, New York, N.Y.) 1976.

[9] Wu X. L., Pine D. J., Chaikin P. M., Huang J. S. and Weitz D. A., *J. Opt. Soc. Am. B*, **7** (1990) 15.

[10] Bicout D. and Maret G., *Physica A*, **210** (1994) 87.

[11] Boas D. A., Campbell L. E. and Yodh A. G., *Phys. Rev. Lett.*, **75** (1995) 1855.

[12] Bicout D., Akkermans E. and Maynard R., *J. Phys. I*, **1** (1991) 471.

[13] Bicout D. and Maynard R., to be published.

[14] Xue J., Pine D. J., Milner S. T., Wu X.-l. and Chaikin P. M., *Phys. Rev. A*, **46** (1992) 6550.